Nanotoxicology

ISSN: 1743-5390 (Print) 1743-5404 (Online) Journal homepage: https://www.tandfonline.com/loi/inan20

# Copper oxide nanoparticles aggravate airway inflammation and mucus production in asthmatic mice via MAPK signaling

Ji-Won Park, In-Chul Lee, Na-Rae Shin, Chan-Mi Jeon, Ok-Kyoung Kwon, Je-Won Ko, Jong-Choon Kim, Sei-Ryang Oh, In-Sik Shin & Kyung-Seop Ahn

**To cite this article:** Ji-Won Park, In-Chul Lee, Na-Rae Shin, Chan-Mi Jeon, Ok-Kyoung Kwon, Je-Won Ko, Jong-Choon Kim, Sei-Ryang Oh, In-Sik Shin & Kyung-Seop Ahn (2016) Copper oxide nanoparticles aggravate airway inflammation and mucus production in asthmatic mice via MAPK signaling, Nanotoxicology, 10:4, 445-452, DOI: 10.3109/17435390.2015.1078851

**To link to this article:** https://doi.org/10.3109/17435390.2015.1078851

http://tandfonline.com/inan
ISSN: 1743-5390 (print), 1743-5404 (electronic)

Nanotoxicology

Nanotoxicology, 2016; 10(4): 445–452
 DOI: 10.3109/17435390.2015.1078851

Taylor & Francis
Taylor & Francis Group

ORIGINAL ARTICLE

# Copper oxide nanoparticles aggravate airway inflammation and mucus production in asthmatic mice via MAPK signaling

Ji-Won Park[1,2]*, In-Chul Lee[3]*, Na-Rae Shin[1], Chan-Mi Jeon[1], Ok-Kyoung Kwon[1], Je-Won Ko[3], Jong-Choon Kim[3], Sei-Ryang Oh[1], In-Sik Shin[3], and Kyung-Seop Ahn[1]

*[1]Natural Medicine Research Center, Korea Research Institute of Bioscience and Biotechnology, Ochang-eup, Cheongwon-gu, Chungju-si, Chungbuk, Republic of Korea, [2]College of Life Science and Biotechnology, Korea University, Seoul, Republic of Korea, and [3]College of Veterinary Medicine, Chonnam National University, Gwangju, Republic of Korea*

**Abstract**

Copper oxide nanoparticles (CuONPs), metal oxide nanoparticles were used in multiple applications including wood preservation, antimicrobial textiles, catalysts for carbon monoxide oxidation and heat transfer fluid in machines. We investigated the effects of CuONPs on the respiratory system in Balb/c mice. In addition, to investigate the effects of CuONPs on asthma development, we used a murine model of ovalbumin (OVA)-induced asthma. CuONPs markedly increased airway hyper-responsiveness (AHR), inflammatory cell counts, proinflammatory cytokines and reactive oxygen species (ROS). CuONPs induced airway inflammation and mucus secretion with increases in phosphorylation of the MAPKs (Erk, JNK and p38). In the OVA-induced asthma model, CuONPs aggravated the increased AHR, inflammatory cell count, proinflammatory cytokines, ROS and immunoglobulin E induced by OVA exposure. In addition, CuONPs markedly increased inflammatory cell infiltration into the lung and mucus secretions, and MAPK phosphorylation was elevated compared to OVA-induced asthmatic mice. Taken together, CuONPs exhibited toxicity on the respiratory system, which was associated with the MAPK phosphorylation. In addition, CuONPs exposure aggravated the development of asthma. We conclude that CuONPs exposure has a potential toxicity in humans with respiratory disease.

**Keywords**

Asthma, copper oxide nanoparticle, MAPKs, respiratory system

**History**

Received 17 October 2014
Revised 6 July 2015
Accepted 08 July 2015
Published online 16 September 2015

## Introduction

Application of nanoparticles has increased in recent decades. Nanoparticles are used in applications such as medical devices, catalysts, cosmetics and microelectronics (Tiede et al., 2009). With this increased application of nanoparticles, concerns have been raised over its potential toxicity to environmental and human health (Nowack et al., 2012). Currently, many researchers have investigated the potential toxicity of nanoparticles using various experiments, including a toxicological assessment study (Elsaesser & Howard, 2012). There are various routes in which nanoparticles may pose a toxic threat to biological systems (Kahru & Ivask, 2013). Previous studies have demonstrated that nanoparticles produce reactive oxygen species (ROS). Overproduction of ROS causes oxidative stress, which can directly destruct cell membrane lipid, proteins and DNA (Winterbourn, 2008). Furthermore, nanoparticles may indirectly produce ROS by disrupting important cell structures, such as the mitochondria (Hsin et al., 2008). Nanoparticles have also recently been shown to directly induce the activation of proinflammatory proteins and transcription factors. These responses eventually lead to an overproduction of proinflammatory mediators, such as cytokines and chemokines, and can result in an extensive inflammatory response in nanoparticle-exposed lesions (Elsaesser & Howard, 2012).

Copper oxide nanoparticles (CuONPs) are metal oxide nanoparticles with wide applications. They have been used in wood preservation and antimicrobial textiles and have the potential to be used as catalysts for carbon monoxide oxidation and as heat transfer fluid in machines (Mortimer et al., 2010). CuONPs can produce comparable amounts of ROS as other nanoparticle do, for example zinc oxide nanoparticles. Due to excess ROS production, CuONPs is considered to have toxic effects on many organs and organisms (Mwaanga et al., 2014). In addition, recent studies have reported that the presentation of CuONPs toxic effects includes the modulation of important transcription factors and proteins expression. Piret et al. (2012) explained that CuONPs increased the abundance of several transcripts coding for transcription factors, such as Nrf-2, NF-κB and AP-1, which in turn regulate the expression of pro-inflammatory interleukins and chemokines. In addition, recent study demonstrated that CuONPs has a strong toxicity in respiratory cells (Cho et al., 2012). CuONPs exhibited potential toxicity in pulmonary-originated cells including A549 cells, and markedly increased proinflammatory mediators and the recruitment of inflammatory cells in bronchoalveolar lavage fluid (BALF).

*These authors contributed equally to this work.

Correspondence: In-Sik Shin, College of Veterinary Medicine, Chonnam National University, 77 Yongbong-ro, Buk-gu, Gwangju 500-757, Republic of Korea. Tel: +82-62-530-2835. Fax: +82-62-530-2809. E-mail: dvmmk79@gmail.com

Kyung-Seop Ahn, Natural Medicine Research Center, Korea Research Institute of Bioscience and Biotechnology, 30 Yeongudanji-ro, Ochang-eup, Cheongwon-gu, Chungju-si, Chungbuk 363-883, Republic of Korea. Tel: +82-43-240-6113. Fax: +82-42-240-6129. E-mail: ksahn@kribb.re.kr

Asthma is characterized by airway inflammation, mucus hypersecretion and airway hyper-responsiveness. The prevalence of allergic asthma has increased in the last decade. The pathogenesis of asthma is a very complex response that is related to various factors, including ROS, cytokines, chemokines and growth factors (Lee et al., 2011). Exposure to external irritants, such as house dust, smoke and pollen, can induce an asthmatic response. Particularly, exposure to chemicals and particles can aggravate asthmatic responses in patients with asthma (Sava et al., 2013). Recent studies have demonstrated that diesel exhaust markedly exacerbated the allergen-induced airway inflammation via elevation of proinflammatory cytokines (Acciani et al., 2013; Lee et al., 2013). Therefore, exposure to specific particles during asthma development is an important risk factor of exacerbation of the asthmatic response.

In this study, we investigated the effects of CuONPs exposure to mice via intranasal instillation on the respiratory system. In addition, we explored the effects of CuONPs exposure on asthma development using the ovalbumin (OVA)-induced asthma murine model.

## Materials and methods

### Test article

The test article examined in this study was commercially available CuONPs purchased from Sigma-Aldrich (544868, St. Louis, MO). Information provides by manufacturer states that the particle size measured by transmission electron microscopy (TEM) is <50 nm. To obtain the size and morphology of the CuONPs, TEM characterization was performed using a JEM-1210 (JEOL, Tokyo, Japan) at an accelerating voltage of 200 kV. The samples were deposited on carbon-coated nickel grids and were air dried overnight before TEM analysis.

### The solubility and hydrodynamic size of CuONPs

Copper oxide nanoparticles (CuONPs) was incubated with PBS (pH 7.4) for 24 h. After incubation, nanoparticle-free supernatants were collected by three rounds of centrifugation at 15 000 × *g* for 30 min. The degree of ionization was evaluated using Nexion 300X inductively coupled plasma-mass spectrometry (ICP-MS; Perkin Elmer, Waltham, MA). The hydrodynamic size of CuONPs was evaluated using Zeta-PSA (ELS-8000, Otsuka Electronic, Tokyo, Japan)

### Experimental procedure for animal experiments

Specific pathogen-free female BALB/c mice (6 weeks old) were purchased from the Koatech Co. (Pyeongtaek, Korea) and used after 2 weeks of quarantine and acclimatization. All experimental procedures were approved by the Institutional Animal Care and Use Committee of the Korea Research Institute of Bioscience and Biotechnology.

The mice were divided into four groups. CuONPs were prepared at 25, 50 and 100 μg/kg doses in 50 μL of PBS. The mice received the CuONPs via intranasal instillation under slight anesthesia for 3 days using Zoletil 50 (Virbac Laboratories, Carros, France). CuONPs was prepared in PBS and sonicated in an ultrasonicator (VCX-130, Sonics and Materials, Newtown, CT) for 3 min (130 W, 20 kHz, pulse 59/1) before intranasal instillation. The normal control group received 50 μL of PBS via intranasal instillation. Airway hyper-responsiveness (AHR) was indirectly assessed 24 h after the final intranasal instillation via single-chamber, whole body plethysmography (Allmedicus, Seoul, Korea). The mice were sacrificed 48 h after the final instillation via an intraperitoneal injection of pentobarbital (50 mg/kg; Hanlim Pharm. Co., Seoul, Korea), and a tracheostomy was performed. To obtain the BALF, ice-cold PBS (0.7 mL) was infused into the lungs two times and withdrawn each time using a tracheal cannula (a total volume of 1.4 mL). The differential cell counts in the BALF were performed using the Diff-Quik® staining reagent (IMEB Inc., San Marcos, CA) according to the manufacturer's instructions. To evaluate CuONPs distribution in lung tissue, the weighed lung tissue (about 100 mg) were digest with concentrated nitric acid overnight, added 30% $H_2O_2$ and then heated in a microwave digestion system (ETHODS One, Milestrone S.r.I., Sorisole, Italy) at 170 °C to remove the remaining nitric acid until the samples were completely digested and became colorless. Finally, remaining solutions were diluted with 2% nitric acid. All samples were analyzed for elemental Cu concentration using Nexion 300X inductively coupled plasma-mass spectrometry (ICP-MS; Perkin Elmer, Waltham, MA).

For investigating the effects of CuONPs on the development of asthma, the mice were divided into five groups. To induce asthma, the mice were sensitized on days 0 and 14 with an intraperitoneal injection of 20 μg of OVA (Sigma-Aldrich) emulsified with 2 mg of aluminum hydroxide (Thermo Scientific, Waltham, MA) in 200 μL of phosphate-buffered saline (PBS, pH 7.4). On days 21, 22 and 23 the mice received 20 μg of OVA and CuONPs (25, 50 and 100 μg/kg) dispersed into 50 μL of PBS via intranasal instillation. The airway responsiveness, BALF sampling and cell staining were performed as described above.

### Measurement of ROS production and contents in BALF

The induction of oxidative stress was monitored using 2′,7′-dichlorofluorescein diacetate (DCF-DA, Molecular Probes, Eugene, OR), which is converted into highly fluorescent DCF by cellular peroxides, including hydrogen peroxide. Briefly, the cells from the BALF were washed with PBS, and the total number of cells ($5 \times 10^3$) was counted. The BALF cells were treated with 20 μM DCF-DA for 10 min at 37 °C. Intracellular ROS activity was evaluated by measuring the fluorescence at 488 nm excitation and 525 nm emission with a fluorescence plate reader (Perkin–Elmer, Waltham, MA). The BALF content was evaluated using a protein assay kit (Bradford assay, Bio-Rad Laboratories, Hercules, CA). The absorbance was measured at 595 nm using an ELISA reader (Molecular Devices, Sunnyvale, CA).

### Measurement of proinflammatory cytokines in the BALF and immunoglobulin E in serum

The levels of IL-1β (BD Biosciences, San Jose, CA), IL-5 (R&D System, Minneapolis, MN), IL-6 (BD Biosciences), IL-13 (R&D System) and TNF-α (BD Biosciences) were measured using commercial ELISA kits according to the manufacturer's protocol. The level of immunoglobulin E in the serum was determined using an ELISA kit (BioLegend, San Diego, CA). The absorbance was measured at 450 nm using an ELISA reader (Molecular Devices).

### Measurement of inflammatory proteins expression in lung tissue

Lung tissue was homogenized (1/10 w/v) using a homogenizer with a tissue lysis/extraction reagent (Sigma-Aldrich) containing a protease inhibitor cocktail (Sigma-Aldrich). Each protein concentration was determined using the Bradford reagent (Bio-Rad Laboratories). Equal amounts of total cellular protein (30 μg) were resolved via electrophoresis using 12% SDS-polyacrylamide gel electrophoresis and transferred to a polyvinyl

difluoride membrane. The membrane was incubated in blocking solution (5% skim milk) followed by incubation overnight at 4 °C in the appropriate primary antibody. The following primary antibodies and dilutions were used: ERK (1:2000 dilution; Cell Signaling, Danvers, MA), pERK (1:1000 dilution; Cell Signaling), JNK (1:1000 dilution; Santa Cruz, Dallas, TX), pJNK (1:1000 dilution; Santa Cruz), p38 (1:1000 dilution; Santa Cruz), p-p38 (1:1000 dilution; Santa Cruz) and β-actin (1:1000 dilution; Cell Signaling). The blots were washed thrice with Tris-buffered saline containing Tween 20 (TBST), and then incubated in a 1:3000 dilution of a horseradish peroxidase (HRP)-conjugated secondary antibody (Jackson Immuno-Research, West Grove, PA) for 30 min at room temperature. The blots were again washed three times with TBST and then were developed using an enhanced chemiluminescence (ECL) kit (Thermo Scientific, Waltham, MA). Densitometric analysis for each protein was determined using Chemi-Doc (Bio-Rad Laboratories).

### Measurement of MMP-9 activity in lung tissue

Protein (30 μg/lane) obtained from lung tissue was loaded for gelatin zymography. Sodium dodecyl sulfate-polyacrylamide gel electrophoresis (SDS-PAGE) zymography was performed to determine the gelatinase activity as described by Heussen and Dowdle (1980). Briefly, the zymogram gels consisted of 10% SDS-PAGE containing 1% gelatin as an MMP substrate. The gels were washed in 2.5% Triton X-100 for 1 h to remove the SDS and then incubated at 37 °C for 16 h in developing buffer (1 M Tris-HCl, pH 7.5 with $CaCl_2$). Thereafter, the gels were stained with 25% methanol/8% acetic acid containing Coomassie brilliant blue. The gelatinase activity was visualized as white bands on a blue background and represented areas of proteolysis.

### Histology and immunohistochemistry

After the BALF samples were collected, the lung tissue was fixed using 4% (v/v) paraformaldehyde. The tissues were paraffin-embedded, sectioned at a thickness of 4 μm and stained using an H&E solution (Sigma-Aldrich) or the periodic acid−Schiff (PAS) solution (IMEB Inc.) to estimate the amount of inflammation or mucus production, respectively. Quantitative analysis of airway inflammation and mucus production was measured using Image analyzer (Molecular Devices). For IHC, the paraffin-embedded sections were deparaffinized, dehydrated, washed using PBS with 0.3% Triton X-100 and incubated for 10 min at room temperature with 10% goat serum to block non-specific staining. Subsequently, slides were incubated overnight at 4 °C with a primary mouse-rabbit MUC5AC antibody (1:100 dilution; Abcam, Cambridge, MA). After removing the primary antibodies, the sections were washed and then incubated with biotinylated secondary antibody at 37 °C for 1 h, followed by incubation with avidin-biotin-peroxidase complex (Vector Laboratories, Burlingame, CA) for 1 h at room temperature. The excess complex was removed and sections were washed with PBS prior to incubation in 0.05% diaminobenzidine (1:200; Millipore Co., Bedford, MA) for a further 10 min. The sections were counterstained, rinsed with PBS to terminate the reaction, and protected with coverslips prior to microscopic examination.

### Statistical analysis

The data are expressed as the means ± standard deviation (SD). Statistical significance was determined using analysis of variance (ANOVA) followed Dunnett's test for multiple comparisons. $p$ values $< 0.05$ were considered to be significant.

## Results

### TEM analysis of CuONPs

Analysis of the vehicle-based solution of CuONPs by TEM indicated a size distribution <50 nm, with a mean and standard deviation of 46.67 ± 17.82 nm (Figure 1). The solubility after 24 h incubation in PBS of CuONPs was 48.75 ± 6.85%. The diameter of CuONPs in PBS was 375.8 ± 140.9 nm.

### Effects of CuONPs on AHR and pathophysiological factors of BALF and serum

The low CuONPs dose group did not show a significant increase in AHR with increasing methylcholine concentrations compared to the vehicle control group. However, the middle and high doses of CuONPs significantly increased AHR compared to the vehicle control group (Figure 2A). CuONPs exposure caused a significant increase in BALF inflammatory cell counts in a dose-dependent manner compared to the vehicle control group (Figure 2B). ROS production, protein content, IL-1β, IL-6 and TNF-α in BALF IL-1 and IgE in the serum were significantly increased in CuONPs nanoparticle exposed groups in a dose-dependent manner (Figure 3).

### Effects of CuONPs on histological alterations and MAPK expression and amount of CuONPs in the lung tissue

Inflammatory cell infiltration and mucus secretion in lung tissue dose-dependently increased in CuONPs exposed groups compared with to the vehicle control group (Supplemental Figure S1). In particular, at the high dose of CuONPs, an extensive inflammatory cell infiltration and mucus secretion were observed in the lung tissue. In addition, CuONPs exposure increased phosphorylation of Erk, JNK and p38 in lung tissue compared to the vehicle control group, which occurred in a dose-dependent manner (Supplemental Figure S2). The concentration of CuONPs in lung tissue was increased in a dose-dependent manner (Supplemental Table S1).

### Effects of CuONPs on AHR and inflammatory cell counts in OVA-induced asthmatic mice

Airway hyper-responsiveness increased in the OVA-induced asthmatic mice. Exposure to CuONPs markedly elevated the AHR compared to the OVA-induced asthmatic mice in a dose-dependent manner (Figure 4A). In addition, OVA-induced

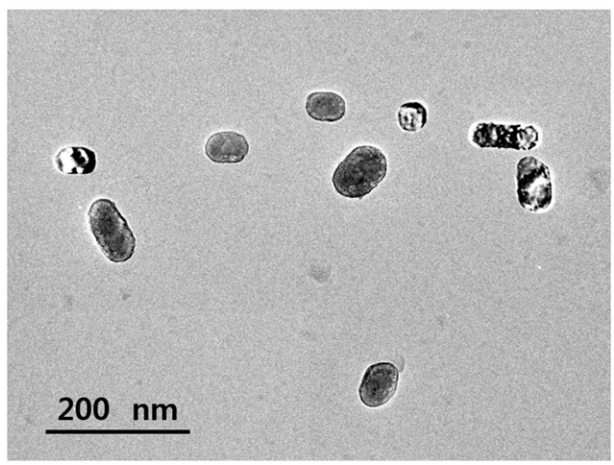


Figure 1. A representative transmission electron micrograph image of CuONPs. The size distribution of CuONPs in suspension (1000 ppm) was measured using a submicron particle size analyzer. The average particle size was 46.67 ± 17.82 nm when measured immediately after preparation.

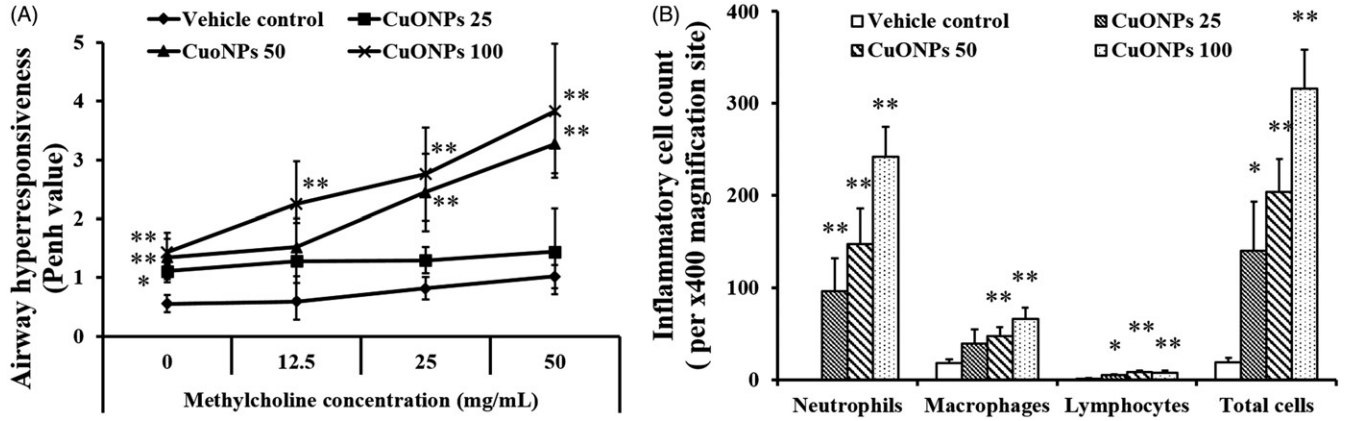


Figure 2. Effects of CuONPs exposure on airway hyper-responsiveness and inflammatory cell counts. (A) Airway hyper-responsiveness. (B) Inflammatory cell counts in BALF. Data represent the mean ± SD, $n = 5$. * $p < 0.05$ and ** $p < 0.01$, respectively, indicate significant differences compared to vehicle controls. Vehicle control, PBS intranasal instillation; CuONPs 25, 50 and 100, CuONPs intranasal instillation (25, 50 and 100 μg/kg, respectively).

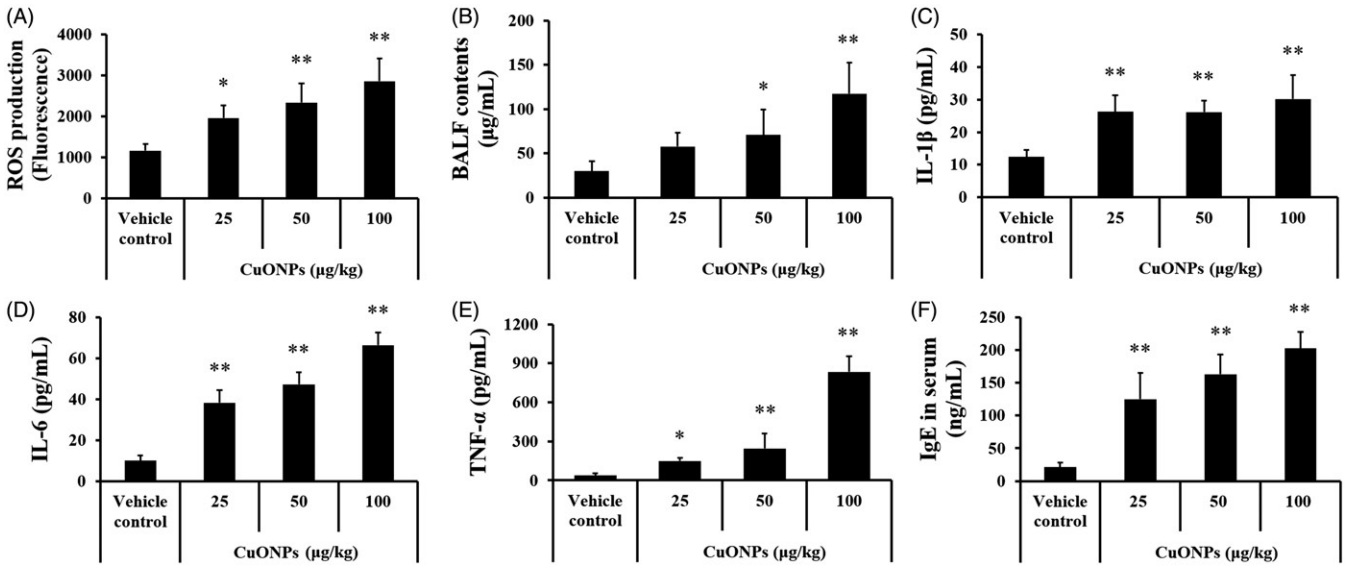


Figure 3. Effects of CuONPs exposure on pathophysiological factors of BALF and serum. (A) ROS production in BALF. (B) BALF contents. (C–E) Levels of IL-1β, IL-6 and TNF-α in BALF, respectively. (F) IgE in serum. Data represent the mean ± SD, $n = 5$. * $p < 0.05$ and ** $p < 0.01$, respectively, indicate significant differences compared to vehicle controls. Vehicle control, PBS intranasal instillation; CuONPs 25, 50 and 100, CuONPs intranasal instillation (25, 50 and 100 μg/kg, respectively).

asthmatic mice had increased inflammatory cell counts in the BALF, particularly eosinophils compared to the vehicle controls. Exposure to CuONPs markedly increased inflammatory cell counts, including eosinophils, neutrophils, macrophages and lymphocytes, compared to the normal control (Figure 4B). These elevations were larger than that observed in the OVA-induced asthmatic mice. In particular, exposure to CuONPs in asthmatic mice significantly increased the number of neutrophils and macrophages compared to the OVA-induced asthmatic mice.

### Effects of CuONPs on pathophysiological factors in BALF and serum in OVA-induced asthmatic mice

Ovalbumin (OVA)-induced asthmatic mice showed increases in ROS production and BALF content compared with to the vehicle controls. CuONPs exposed mice also showed increases in ROS production and BALF content in a dose-dependent manner, and these increases were higher than those observed in the OVA-induced asthmatic mice (Figure 5A and B, respectively). The production of IL-6 and TNF-α increased in OVA-induced asthmatic mice. Exposure to CuONPs further increased IL-6 and TNF-α production compared to the OVA-induced asthmatic mice (Figure 5C and D, respectively). Production of the Th2 cytokines IL-5 and IL-13 was consistent with the results found for IL-6 and TNF-α. Exposure to CuONPs elevated the production of IL-5 and IL-13 to a greater extent than that observed in the OVA-induced asthmatic mice (Figure 5E and F, respectively). A greater increase in OVA-specific IgE was also observed in CuONPs exposed mice compared to the OVA-induced asthmatic mice (Figure 5G).

### Effects of CuONPs on airway inflammation and mucus secretion in OVA-induced asthmatic mice

Ovalbumin (OVA)-induced asthmatic mice had increased airway inflammation compared to the vehicle controls (Figure 6A and B). CuONPs exposed mice also showed a marked increase in airway inflammation in a dose-dependent manner, and this increase was higher than that observed in OVA-induced asthmatic mice. Mucus

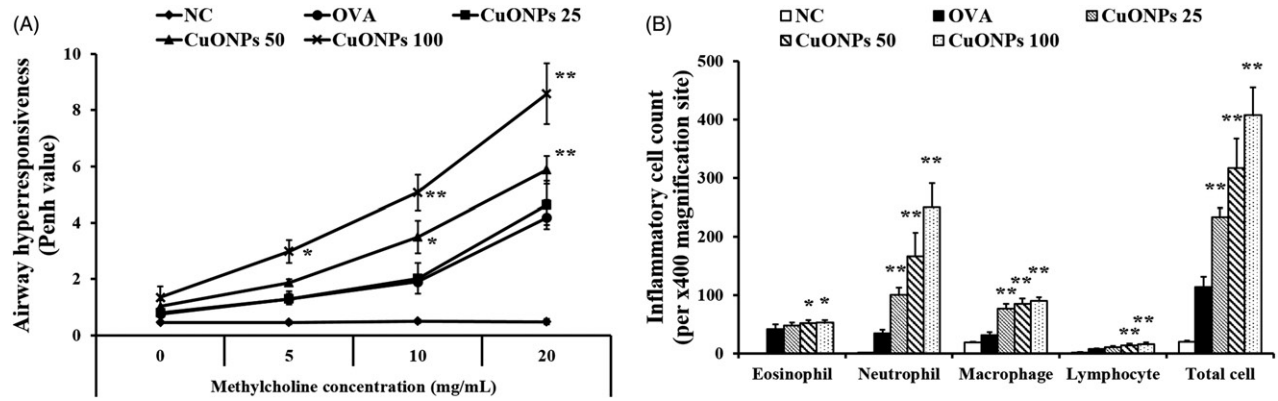


Figure 4. Effects of CuONPs exposure on airway hyper-responsiveness and inflammatory cell counts in OVA-induced asthmatic mice. (A) Airway hyper-responsiveness. (B) Inflammatory cell counts in BALF. Data represent the mean ± SD, $n = 5$. *$p < 0.05$ and **$p < 0.01$, respectively, indicate significant differences compared to OVA. Vehicle control, PBS intranasal instillation; OVA, OVA intranasal instillation (50 μg/mouse); CuONPs 25, 50 and 100, OVA (50 μg/mouse) + CuONPs intranasal instillation (25, 50 and 100 μg/kg, respectively).

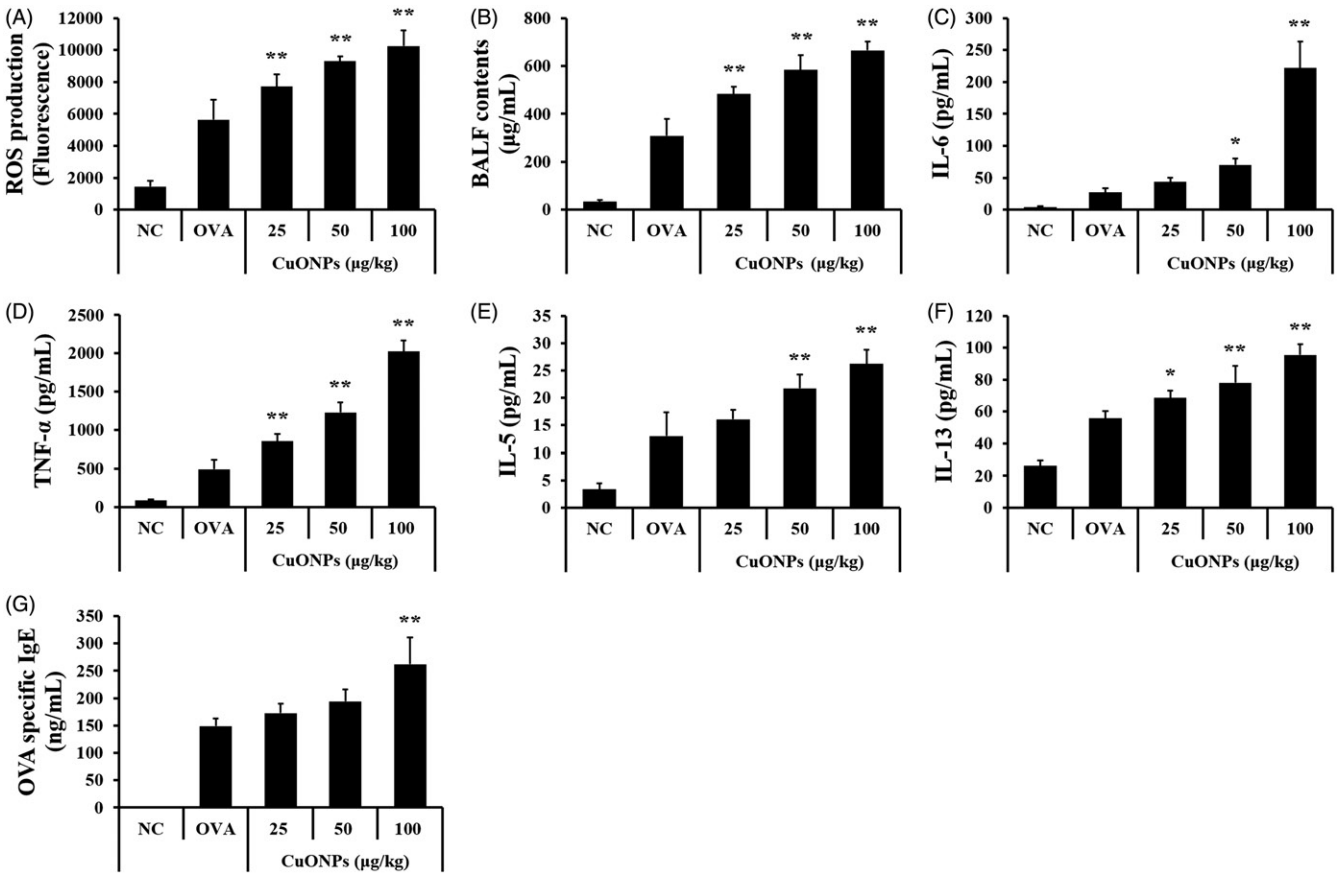


Figure 5. Effects of CuONPs exposure on pathophysiological factors of BALF and serum in OVA-induced asthmatic mice. (A) ROS production in BALF. (B) BALF contents. (C–F) levels of IL-6, TNF-α, IL-5 and IL-13 in BALF, respectively. (G) OVA-specific IgE in serum. Data represent the mean ± SD, $n = 5$. *$p < 0.05$ and **$p < 0.01$, respectively, indicate significant differences compared to OVA. Vehicle control, PBS intranasal instillation; OVA, OVA intranasal instillation (50 μg/mouse); CuONPs 25, 50 and 100, OVA (50 μg/mouse) + CuONPs intranasal instillation (25, 50 and 100 μg/kg, respectively).

secretion was increased in OVA-induced asthmatic mice. Exposure to CuONPs further increased mucus secretion compared to the OVA-induced asthmatic mice (Figure 6A and C). The observed MUC5AC expression was consistent with the results observed for airway inflammation and mucus secretion. CuONPs exposed mice significantly increased the expression of MUC5AC in a dose-dependent manner compared to the OVA-induced asthmatic mice (Figure 6A and D).

### Effects of CuONPs on MAPKs and MMP-9 in OVA-induced asthmatic mice

The phosphorylation of the MAPKs Erk, JNK and p38 was elevated in OVA-induced asthmatic mice compared to the vehicle controls. CuONPs exposed mice showed a further increase in the phosphorylation of MAPKs compared to the OVA-induced asthmatic mice (Figure 7A and B). The MMP-9

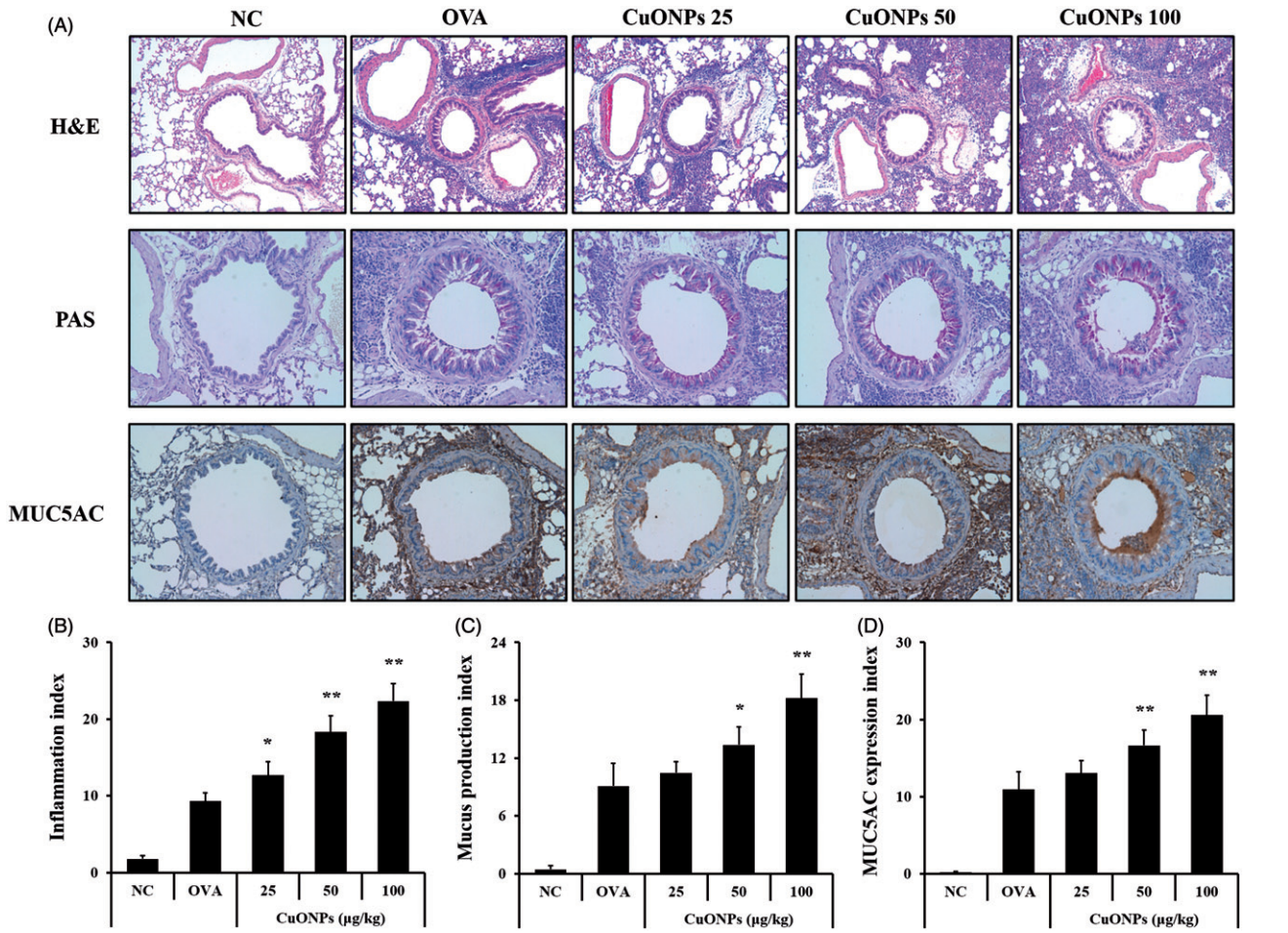


Figure 6. Effects of CuONPs exposure on inflammatory responses, mucus secretion and MUC5AC expression in lung tissue from OVA-induced asthmatic mice. (A) Representative figure of inflammatory responses, mucus secretion and MUC5AC expression in lung tissue. (B,C) Quantitative analysis of inflammatory responses, mucus secretion and MUC5AC expression in lung tissue, respectively. Data represent the mean ± SD, $n = 5$. *$p < 0.05$ and **$p < 0.01$, respectively, indicate significant difference compared to OVA. Vehicle control, PBS intranasal instillation; OVA, OVA intranasal instillation (50 μg/mouse); CuONPs 25, 50 and 100, OVA (50 μg/mouse) + CuONPs intranasal instillation (25, 50 and 100 μg/kg, respectively).

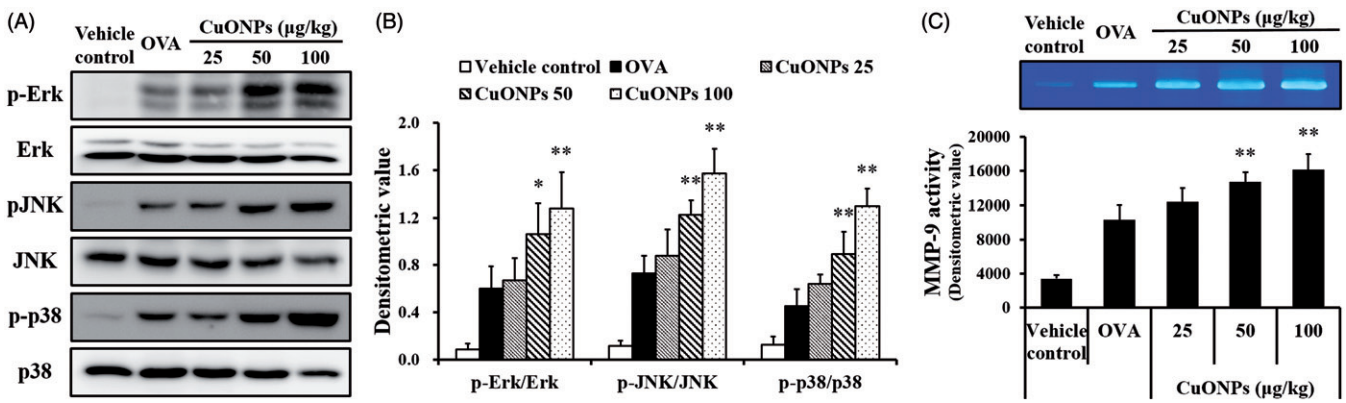


Figure 7. Effects of CuONPs exposure on MAPK phosphorylation and MMP-9 activity in lung tissue from OVA-induced asthmatic mice. (A) MAPK expression on gels. (B) Quantitative analysis of protein expression. (C) MMP-9 activity. Data represent the mean ± SD, $n = 5$. *$p < 0.05$ and **$p < 0.01$, respectively, indicate significant differences compared to OVA. Vehicle control, PBS intranasal instillation; OVA, OVA intranasal instillation (50 μg/mouse); CuONPs 25, 50 and 100, OVA (50 μg/mouse) + CuONPs intranasal instillation (25, 50 and 100 μg/kg, respectively).

activity results were similar to the results observed for MAPKs. MMP-9 activity, which is a crucial factor in the development of asthma, increased in OVA-induced asthmatic mice. Exposure to CuONPs further increased MMP-9 activity in a dose-dependent manner compared to the OVA-induced asthmatic mice (Figure 7C).

## Discussion and conclusions

Currently, increased amounts of different nanoparticles are produced, and their production is projected to become a $2.4 trillion market by 2015 (Hu et al., 2014). Due to increases in nanoparticle applications and production, their release is

continuously elevated in the environment, and in particular, marked increases are observed in factories where they are manufactured and in nearby surroundings (Nowack et al., 2012). Although nanoparticles have many properties and applications, the potential toxicity caused by nanoparticle exposure has become a major concern to the community. CuONPs, a metal oxide nanoparticle, is often used as an industrial catalyst or to improve a product's functional properties (Mortimer et al., 2010). Factory workers are exposed to higher CuONPs doses than other people. To date, limited toxicity data on CuONPs are available. Some experiments have demonstrated that CuONPs is potentially toxic to the respiratory system (Kumar & Nagesha, 2013). However, there have been no studies investigating the mechanisms involved in the respiratory toxicity induced following CuONPs exposure.

Exposure to CuONPs induced airway inflammation with increases in proinflammatory cytokines and ROS. CuONPs markedly increased the number of neutrophils in BALF in a dose-dependent manner. Neutrophils contain various stimulatory mediators, such as ROS, proinflammatory cytokines and tissue lysis enzymes, which not only aggravate neutrophilic airway inflammation but also destroy normal alveolar structure, results the loss of lung functions (Grommes & Soehnlein, 2011; Profita et al., 2010). Our findings are similar to the results observed in previous study. Kumar and Nagesha (2013) reported that CuONPs induces neutrophilic airway inflammation and increases ROS production. In addition, airway inflammation and mucus secretion is associated with elevated AHR. Previous studies have demonstrated that inflammatory cells, such as neutrophils and eosinophils, increase AHR and mucus secretion, thereby inhibiting normal airflow in the airway. In this study, CuONPs exposure significantly increased AHR compared with the vehicle controls. These results indicate that CuONPs exposure induces neutrophilic airway inflammation and limits normal lung functions. Exposure to CuONPs increased the phosphorylation of the MAPKs Erk, JNK and p38 in lung tissue. The phosphorylation of MAPKs is a critical step in the molecular pathway signaling of inflammatory response and mucus production. Phosphorylation of MAPKs can be induced production of proinflammatory cytokines and MUC5AC (Busse et al., 2005; Casalino-Matsuda et al., 2006; Hewson et al., 2004; Shao et al., 2004). Thus, the mechanism of CuONPs toxicity is thought to involve the phosphorylation of MAPKs. In our experiments, exposure to CuONPs elevated the proinflammatory cytokines IL-1β, IL-6 and TNF-α and mucus production and a concomitant increase in the phosphorylation of MAPKs was observed. These results further support the idea that the potential toxicity of CuONPs involves the phosphorylation of MAPKs.

Asthma is characterized by eosinophilic airway inflammation, AHR and mucus overproduction. Asthma is recognized as a major public health problem and its prevalence has substantially increased over recent decades (Welte & Groneberg, 2006). Asthma is induced by the inhalation of allergens such as pollens, house dust, inhalants and air pollutants (Holgate, 2008). In the development of asthma, eosinophils are closely involved and the presence of eosinophils in the airway is considered as a defining feature of asthma (Lee et al., 2011). Eosinophils have a rich source of cytotoxic proteins, lipid mediator, ROS and cytokines, which cause damage to epithelial cells, mucus secretion and AHR (Possa et al., 2013). In this study, OVA-induced asthmatic mice exhibited a marked increased number of eosinophils compared with the normal controls. However, CuONPs-treated mice increased the eosinophil count with elevation of other inflammatory cells compared with the OVA-induced asthmatic mice. These findings indicated that the exposure to CuONPs aggravates the eosinophilia induced by OVA challenge.

Inflammatory cells are activated by proinflammatory cytokines and they, in turn, produce ROS, lipid mediators, growth factors and cytokines (Piret et al., 2012). In previous study, asthmatic mice showed the significant increases in eosinophil counts, proinflammatory cytokines such as IL-4, IL-5 and IL-13 with elevation of IgE level compared with normal mice. These features are considered as important indicators (Shin et al., 2014). The proinflammatory cytokines cause pathophysiological responses, including eosinophilic airway inflammation, smooth muscle contraction and mucus production, which eventually result in airway obstruction and AHR (Hansbro et al., 2011). These roles of proinflammatory cytokines in asthma have been proved by many *in vivo* experiment and clinical trials (Lee et al., 2011; Singh et al., 2010). In this study, OVA-induced asthmatic mice showed increases in the numbers of inflammatory cells in BALF, as well as an elevation in the proinflammatory cytokines IL-5, IL-13, IL-6 and TNF-α. CuONPs exposed mice showed an even greater increase in these pathophysiological factors than the OVA-induced asthmatic mice. Furthermore, CuONPs exposed mice had a greater increase in neutrophils than eosinophils when compared to the OVA-induced asthmatic mice. These increases were accompanied with elevated AHR in CuONPs exposed mice compared to the OVA-induced asthmatic mice. Thus, deterioration of the asthmatic condition by CuONPs is considered to result from the increased number of neutrophils generated in these mice. The results from histological analysis were consistent with the pathophysiological results found for the BALF. CuONPs exposed mice showed extensive airway inflammation, mucus production and overexpression of MUC5AC in the lung tissue compared to the OVA-induced asthmatic mice. In addition, the phosphorylation of the MAPKs Erk, JNK and p38 was increased more in CuONPs exposed mice than the OVA-induced asthmatic mice. MAPK signaling is known as an important pathway in the pathogenesis of asthma (Pelaia et al., 2005). In the development of asthma, phosphorylation of MAPKs induced activation of various transcription factors, which eventually produced proinflammatory cytokines, chemokines, adhesion molecules, mucin and matrix metalloproteins, resulting in asthmatic responses (Alam & Gorska, 2011; Atherton et al., 2003; Liu et al., 2008). In clinical trial, increases in MAPK phosphorylation were observed in airway biopsy samples from asthmatic patients (Liu et al., 2008). Inhibition of MAPK phosphorylation reduces asthmatic responses in several *in vivo* experiments (Alam & Gorska, 2011; Kim et al., 2012; Tachdjian et al., 2009). In this study, CuONPs exposed mice more had a greater increase in proinflammatory cytokines, MMP-9 activity and MUC5AC expression, as well as led to an increase in MAPK phosphorylation. Based on these findings, CuONPs exposure in asthmatic conditions may accelerate the development of asthma, and this effect may be related to increased phosphorylation of MAPKs.

Overall, exposure to CuONPs induced airway inflammation, AHR and mucus secretion with increases in inflammatory mediators under normal lung conditions. In asthmatic conditions, exposure to CuONPs augmented the production of inflammatory cells and mediators, and exacerbated asthmatic responses, an effect which involved MAPK phosphorylation. Due to the potential toxicity of CuONPs, people with respiratory diseases must be careful with CuONPs exposure.

## Declaration of interest

There are no competing financial interests. This research was supported by a grant from the KRIBB Research Initiative program (KGM 1221521) of the Republic of Korea.

## References


Acciani TH, Brandit EB, Khurana Hershey GK, Le Cras TD. 2013. Diesel exhaust particle exposure increases severity of allergic asthma in young mice. Clin Exp Allergy 43:1406–18.

Alam R, Gorska MM. 2011. Mitogen-activated protein kinase signaling and ERK1/2 bistability in asthma. Clin Exp Allergy 41:149–59.

Atherton HC, Jones G, Danahay H. 2003. IL-13-induced changes in the goblet cell density of human bronchial epithelial cell cultures: MAP kinase and phosphatidylinositol 3-kinase regulation. Am J Physiol Lung Cell Mol Physiol 285:L730–9.

Busse PJ, Zhang TF, Srivastava K, Lin BP, Schofield B, Sealfon SC, et al. 2005. Chronic exposure to TNF-alpha increases airway mucus gene expression in vivo. J Allergy Clin Immunol 116:1256–63.

Casalino-Matsuda SM, Monzon ME, Forteza RM. 2006. Epithermal growth factor receptor activation by epithermal growth factor mediates oxidant-induced goblet cell metaplasia in human airway epithelium. Am J Respir Cell Mol Biol 34:581–91.

Cho WS, Duffin R, Poland CA, Duschl A, Oostingh GJ, Macnee W, et al. 2012. Differential pro-inflammatory effects of metal oxide nanoparticles and their soluble ions in vitro and in vivo; zinc and copper nanoparticles, but not their ions, recruit eosinophils to the lung. Nanotoxicology 6:22–35.

Elsaesser A, Howard CV. 2012. Toxicology of nanoparticles. Adv Drug Deliv Rev 64:129–37.

Grommes J, Soehnlein O. 2011. Contribution of neutrophils to acute lung injury. Mol Med 17:293–307.

Hansbro PM, Kaiko GE, Foster PS. 2011. Cytokine/anticytokines therapy – novel treatments for asthma. Brit J Pharmacol 163:81–95.

Heussen C, Dowdel EB. 1980. Electrophoretic analysis of plasminogen activators in polyacrylamide gels containing sodium dodecyl sulfate and copolymerized substrate. Anal Biochem 102:196–202.

Hewson CA, Edbrooke MR, Johnston SL. 2004. PMA induces the MUC5AC respiratory mucin in human bronchial epithelial cells, via PKC, EGF/TGF-alpha, Ras/Raf, MEK, ERK and Sp1-dependent mechanism. J Mol Biol 344:683–95.

Holgate ST. 2008. The airway epithelium is central to the pathogenesis of asthma. Allergol Int 57:1–10.

Hsin YH, Chena CF, Huang S, Shih TS, Lai PS, Cheuh PJ. 2008. The apoptotic effect of nanosilver is mediated by a ROS and JNK-dependent mechanism involving the mitochondrial pathway in NIH3T3 cells. Toxicol Lett 179:130–9.

Hu W, Culloty S, Darmody G, Lynch S, Davenport J, Ramirez-Garcia S, et al. 2014. Toxicity of copper oxide nanoparticles in the blue mussel, *Mytilus edulis*: a redox proteomic investigation. Chemosphere 108: 289–99.

Kahru A, Ivask A. 2013. Mapping the dawn of nanoecotoxicological research. Acc Chem Res 46:823–33.

Kim SR, Lee KS, Park SJ, Jeon MS, Lee YC. 2012. Inhibition of p38 MAPK reduce expression of vascular endothelial growth factor in allergic airway disease. J Clin Immunol 32:574–86.

Kumar R, Nagesha DK. 2013. Size-dependent study of pulmonary responses to nano-sized iron and copper oxide nanoparticles. Methods Mol Biol 1028:247–64.

Lee GB, Brandt EB, Xiao C, Gibson AM, Le Cras TD, Brown LA, et al. 2013. Diesel exhaust particles induce cysteine oxidation and s-glutathionylation in house dust mite induced murine asthma. PLoS One 8:e60632.

Lee MY, Seo CS, Lee JA, Lee NH, Kim JH, Ha H, et al. 2011. Anti-asthmatic effects of angelica dahurica against ovalbumin-induced airway inflammation via upregulation of heme oxygenase-1. Food Chem Toxicol 49:829–37.

Liu W, Liang Q, Balzar S, Wenzel S, Gorska M, Alam R. 2008. Cell-specific activation profile of extracellular signal-regulated kinase 1/2, Jun N-terminal kinase, and p38 mitogen-activated protein kinases in asthmatic airways. J Allergy Clin Immunol 121:893–902.

Mortimer M, Kasemets K, Kahru A. 2010. Toxicity of ZnO and CuO nanoparticles to ciliated protozoa *Tetrahymena thermophila*. Toxicology 269:182–9.

Mwaanga P, Carraway ER, van den Hurk P. 2014. The induction of biochemical changes in Daphnia magna by CuO and ZnO nanoparticles. Aquat Toxicol 150:201–9.

Nowack B, Ranville JF, Diamond S, Gallego-Urrea JA, Metcalfe C, Rose J, et al. 2012. Potential scenarios for nanomaterial release and subsequent alteration in the environment. Environ Toxicol Chem 31: 50–9.

Pelaia G, Cuda G, Vatrella A, Gallelli L, Caraglia M, Marra M, et al. 2005. Mitogen-activated protein kinases and asthma. J Cell Physiol 202:642–53.

Piret JP, Jacques D, Audinot JN, Mejia J, Boilan E, Noel F, et al. 2012. Copper(II) oxide nanoparticles penetrate into HepG2 cells, exert cytotoxicity via oxidative stress and induce pro-inflammatory response. Nanoscale 4:7168–84.

Possa SS, Leick EA, Prado CM, Martins MA, Tiberio IF. 2013. Eosinophilic inflammation in allergic asthma. Front Pharmacol 4:46.

Profita M, Sala A, Bonanno A, Riccobono L, Ferraro M, La Grutta S, et al. 2010. Chronic obstructive pulmonary disease and neutrophil infiltration: role of cigarette smoke and cyclooxygenase products. Am J Physiol Lung Cell Mol Physiol 298:L262–9.

Sava F, MacNutt MJ, Carlsten CR. 2013. Nasal neurogenic inflammation markers increase after diesel exhaust inhalation in individuals with asthma. Am J Respir Crit Care Med 188:759–60.

Shao MX, Nakanaga T, Nadel JA. 2004. Cigarette smoke induces MUC5AC mucin overproduction via tumor necrosis factor-alpha-converting enzyme in human airway epithelial (NCI-H292) cells. Am J Physiol Lung Cell Mol Physiol 287:L420–7.

Shin IS, Park JW, Shin NR, Jeon CM, Kwon OK, Kim JS, et al. 2014. Melatonin reduces airway inflammation in ovalbumin-induced asthma. Immunobiology 219:901–8.

Singh D, Kane B, Molfino NA, Faggioni R, Roskos L, Woodcock A. 2010. A phase 1 study evaluating the pharmacokinetics, safety and tolerability of repeat dosing with a human IL-13 antibody (CAT-354) in subjects with asthma. BMC Pulm Med 10:3.

Tachdjian R, Mathias C, Al Khatib S, Bryce PJ, Kim HS, Blaeser F, et al. 2009. Pathogenicity of a disease-associated human IL-4 receptor allele in experimental asthma. J Exp Med 206:2191–204.

Tiede K, Hasselly M, Breitbarth E, Chaudhry Q, Boxall ABA. 2009. Considerations for environmental fate and ecotoxicity testing to support environmental risk assessments for engineered nanoparticles. J Chromatogr Part A 1216:503–9.

Welte T, Groneberg DA. 2006. Asthma and COPD. Exp Toxicol Pathol 2: 35–40.

Winterbourn C. 2008. Reconciling the chemistry and biology of reactive oxyten species. Nat Chem Biol 4:278–86.


## Supplementary material available online

Supplementary Figures S1 and S2, and Table S1